Optics Communications 344 (2015) 156–160

Contents lists available at ScienceDirect

Optics Communications

journal homepage: www.elsevier.com/locate/optcom

Tunable Fabry–Perot filter in cobalt doped fiber formed by optically heated fiber Bragg gratings pair

Ying Li [a,b], Bin Zhou [a,c,*], Liang Zhang [a,b], Sailing He [a,b]

[a] ZJU-SCNU Joint Research Center of Photonics, South China Normal University, Guangzhou 510006, PR China
[b] Centre for Optical and Electromagnetic Research, State Key Laboratory of Modern Optical Instrumentation, Zhejiang University, Hangzhou 310058, PR China
[c] South China Academy of Advanced Optoelectronic, South China Normal University, Guangzhou 510006, PR China

ARTICLE INFO

Article history:
Received 2 November 2014
Received in revised form
12 January 2015
Accepted 13 January 2015
Available online 14 January 2015

Keywords:
Fabry–Perot filter
Fiber Bragg grating pair
Cobalt doped fiber

ABSTRACT

In this paper, a tunable fiber Fabry–Perot (F–P) filter by *all-optical heating* is proposed. Two high reflective fiber Bragg gratings (FBG) fabricated in cobalt doped single mode fiber form the F–P cavity. The cobalt-doped fiber used here is an active fiber, and it transforms optical power from a control laser into heat effectively due to the nonradiative processes. The generated heat raises the refraction index of the fiber and enlarges the F–P cavity's length, realizing the all-optical tuning characteristics. By adjusting the power of the control laser, the resonant wavelength of our proposed fiber F–P filter can be high precisely controlled. The cavity length of the filter is carefully designed to make sure the longitude mode spacing is comparable to the grating bandwidth, making it single mode operating.

1. Introduction

Fabry–Perot (F–P) cavity based filters and interferometers are providing the highest known optical wavelength resolution for more than 100 years. Optical fiber F–P filters with tiny size are one of the most important fiber devices in the fiber communication, fiber sensing and some other applications, due to its ultra-narrow resonance peaks and is more desirable for high accuracy wavelength measurement [1–9]. Most of the fiber F–P cavities are unadjustable and their cavity lengths are fixed once been fabricated. However, a tunable device is always much more flexible than a fixed one, in the applications such as wavelength interrogation, the F–P resonant peak is required to sweep repeatedly. The most popular way in forming a tunable fiber F–P cavity is to change its cavity length mechanically, such as driven by a piezoelectric transducer (PZT) [10,11]. Although the mechanical way is popular for its high speed and high resolution, it also has its deficiencies: one is the hysteresis due to which the wavelength–voltage relationship of an F–P filter is nonreciprocal when driven by a PZT actuator [12,13], another one is the relatively short life time of a mechanical structure. Instead of mechanically controlling, in this paper we managed to design a tunable fiber F–P filter by all-optical heating. An attractive feature of the proposed approach is that it is readily tunable by a controlling laser and will make the filter of considerable interest as wavelength-selective device in many applications.

The fiber F–P filter we proposed is based on FBGs pair (FBGP), which is fabricated in a cobalt-doped single mode optical fiber. The element cobalt can absorb the energy from the controlling laser, and transform it into heat effectively due to the nonradiative processes [14]. The generated heat raises the temperature and the refraction index of the fiber, and ultimately enlarges the F–P cavity length, leading to the shift of the resonant wavelength which can be monitored by an optical spectrum analyzer (OSA). Owing to the cobalt-doped optical fiber, we can control the resonant wavelength of the fiber F–P filter easily by adjusting the power of the heating laser. We were doing the experiment for periods of days, there's no significant decay or degradation of the filter, showing the stability of this proposed device.

In addition, except for heating the FBGs from inside out using the cobalt doped fiber, heaters can also be made at the surface of the fiber, such as thin film heaters [15–17]. One significant advantage of the thin film heaters is the temperature distribution along the FBGs, i.e., the spectrum of the FBGs can be arbitrary controlled by carefully designing the films' thickness, shape and length, which is difficult in the cobalt fiber. However, in heating the cobalt fiber, no electrode and metallic material are required. Furthermore the remote controlling is also possible as its all-optical heating property, which makes it practical in harsh environment and immunity to the electromagnetic interference.

* Corresponding author at: Higher Education Mega Center Campus, South China Academy of Advanced Optoelectronic, South China Normal University, Guangzhou 510006, PR China
E-mail address: zhoubin_mail@163.com (B. Zhou).

http://dx.doi.org/10.1016/j.optcom.2015.01.041
0030-4018/

2. Configuration and principle

The schematic diagram of the experiment for testing the tunable fiber F–P filter is shown in Fig. 1. The key component is a 3 cm long cobalt doped single mode fiber (CorActive Ltd., attenuation: 1 dB/cm from 1250 to 1620 nm, cobalt is doped in the fiber core). Both ends of the cobalt doped fiber are spliced to the ordinary communication single mode fibers. Two adjacent FBGs fabricated in the cobalt doped fiber forms the F–P filter. In order to achieve the single mode operation, the free space range (FSR) of the F–P cavity and the bandwidth of the FBG should be comparable. The FBG's bandwidth is typically in the order of a few tenths nanometers, thus the adjacent distance of the FBGs should be carefully designed. The numbers of longitude mode supported by the cavity is mainly determined by the mode spacing, which is given by [18]

$$\Delta\lambda = \frac{\lambda^2}{2nL_{eff}} \tag{1}$$

where λ is the wavelength, n is the effective refraction index of the fiber, L_{eff} is effective length of the F–P cavity which is defined as [16]:

$$L_{eff} = d + L_{eff1} + L_{eff2} \tag{2}$$

where d is end to end distance of the two gratings (shown in Fig. 1), and $L_{eff1,2}$ are the effective lengths of the two gratings which are given by [19]:

$$L_{eff} = L\frac{\sqrt{R}}{2\mathrm{atanh}(\sqrt{R})} \tag{3}$$

where L (shown in Fig. 1) and R are the length and reflectivity of the FBG, respectively. For a uniform FBG, the reflectivity can be described as: $R = \tan h^2(\pi n_1 L/\lambda_0)$, where n_1 is the refraction index change of the FBG, i.e. the FBG's amplitude. Thus once the FBG's amplitude n_1 is fixed, the FSR of the FBGP formed fiber F–P cavity is depends on the adjacent distance of FBGs d and FBG length L.

The FBG bandwidth is also depends on the FBG's amplitude n_1 and FBG length L. In order to achieve the single longitudinal mode operation, it is necessary to make the FSR of the F–P cavity comparable with the bandwidth of the FBGs which form the F–P cavity. Before fabricating the FBGP based F–P cavity, we checked the relationship of these two parameters carefully both by simulation and experiment in order to guide the design, and the results are shown in Fig. 2. We fabricated a 2 mm long FBG with −13.89 dB transmission dip in the spectrum on the cobalt doped fiber. We use the software Optiwave (the OptiGrating module) for simulation. Fig. 2a shows the simulated and measured transmission

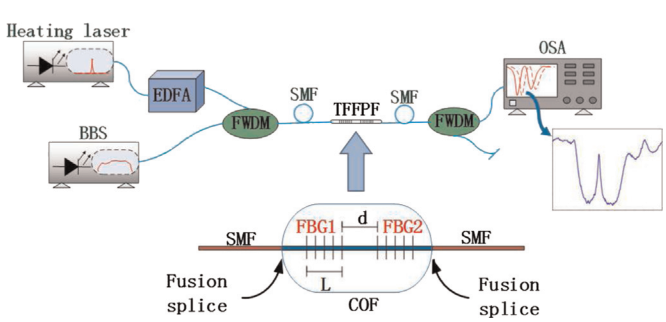

Fig. 1. The schematic diagram of the experiment for testing the tunable fiber F–P filter (TFFPF). Heating laser is used to heat the cobalt-doped optical fiber; BBS, broadband light source; OSA, optical spectrum analyzer; SMF, single mode fiber; FBG, fiber Bragg grating; FWDM, filter wavelength division multiplexer (two channels: transmission channel, 1550 ± 10 nm; reflection channel, 1260～1610 nm except 1550±10 nm); EDFA, erbium doped fiber amplifier; L is the length of the FBG; d is the distance between the two FBGs (end to end). The inset is the transmission spectra of the F–P filter.

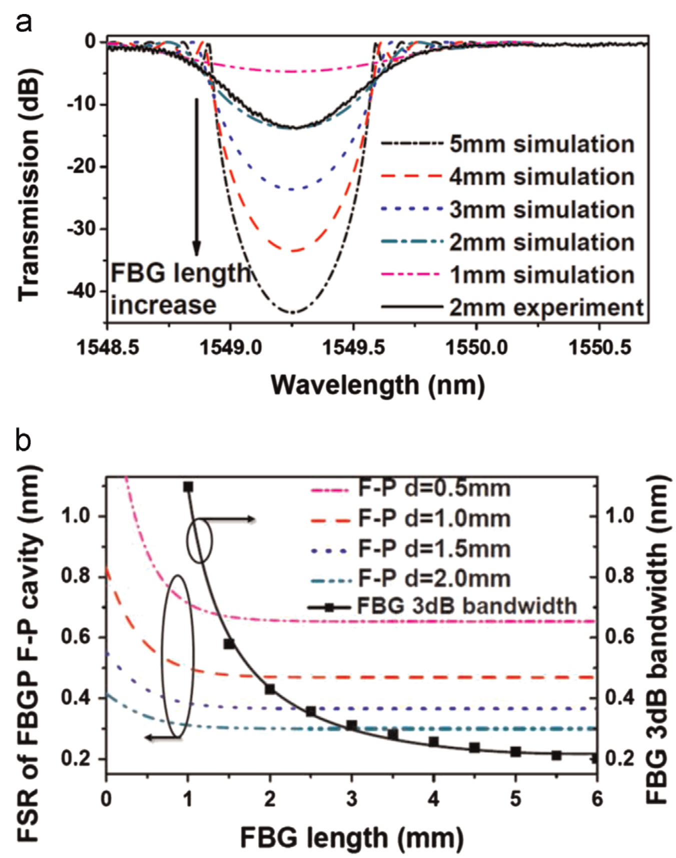

Fig. 2. The FSR of the FBGP formed F–P cavity compares with the bandwidth of the FBGs which form the F–P cavity. (a) Measured and simulated FBG transmission spectra with different FBG lengths. (b) The FSR of F–P cavity with different d and L described in Eq. 2, and the FBG's 3 dB bandwidth.

spectra of FBGs with the same parameters (FBG's amplitude n_1 and period) and difference grating lengths. The grating amplitude n_1 is set to be 6.4×10^{-4} in the simulate so as to match the experiment result, see the measured spectrum of the 2 mm long FBG in Fig. 2a.

Once n_1 is chosen, the only parameters dominate the F–P cavity are L and d. The left axis of Fig. 2b shows the FSR of the F–P cavities with different d decreases as the FBG length L increases. It seems the FSR has a lower limit when the FBG length L tends to infinity. The right axis of Fig. 2b shows the 3 dB bandwidth of the FBG which forms the F–P cavity. It is clearly from Fig. 2 the decline rate of the FBG's 3 dB bandwidth is faster than the FSR of the F–P cavity. In order to achieve single mode operation of the filter, the FBG's length should be longer than 1.40, 1.85, 2.35, 2.95 mm while d is 0.5, 1.0, 1.5, 2.0 mm, respectively.

The longer the FBG is, the narrower the bandwidth and the higher the reflectivity are, as shown in Fig. 2a. It seems that the FBG of longer length is easier to realize the single longitudinal mode operation. However, the length of the FBG in our scheme is not the longer the better. It is limited by the non-uniform heating in the cobalt doped fiber: as the absorption coefficient is big (1 dB/cm) in our experiment, the heating laser power decays along the cobalt doped fiber and the generated heat is not uniform. The temperature distribution along this fiber would also be non-uniform which would lead to the distortion of the FBG fabricated on it. Fig. 3 shows the reflection spectra distortion of gratings with different lengths (3 mm and 5 mm) at an increasing heating laser power. When the laser power increases from 0 to 300 mW, both FBGs become chirped fiber gratings, and the situation of 5 mm long FBG is much worse than that of the 3 mm long FBG. Thus considering the results from Figs. 2 and 3, the FBG's length L and the spacing d is determined to be 2 mm and 1 mm in our

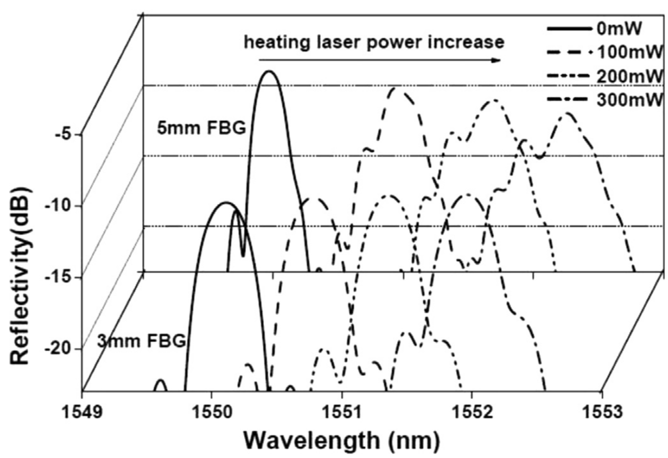

Fig. 3. The reflection spectra distortion of the FBGs with different grating length and heated at different heating power levels (experiment results). (a) 3 mm FBG, (b) 5 mm FBG heated using 0 mW, 100 mW, 200 mW and 300 mW heating laser, respectively.

experiment, respectively.

The filter wavelength division multiplexer (FWDM, shown in Fig. 1) used here has three ports: a transmission port, a reflection port and a common port. When a broadband light (1260–1610 nm) injects into the common port, the filtered light (1540–1560 nm) comes out from the transmission port and the remaining light comes out from the reflection port, and vice versa, the FWDM can combine the light from the transmission and reflection channels with the wavelength value mentioned above and finally into the common channel. In our experiments, a tunable laser and an erbium doped fiber amplifier (EDFA) are used to heat the cobalt doped fiber. The wavelength of the tunable heating laser is set to be 1520 nm which is within the gain range of the EDFA, and the FBGs reflective wavelength is around 1550 nm, thus they are at two different channels of the FWDMs used here. The output power of the broadband light source (BBS) is less than 10 mW. It is much smaller than the heating power from the EDFA and won't interference the heating process. The BBS serves as a signal source. As is shown in the Fig. 1, the left FWDM couples the BBS and the heating laser together, and the right FWDM splits the heating laser away, to prevent the damage to the OSA. The transmission spectrum of the F–P filter is received by a high precision OSA (AP205x-A series optical spectrum analyzer, APEX technologies). In the inset spectrum of Fig. 1, there is only one longitude mode within the grating bandwidth. The F–P filter's 3 dB bandwidth is measured to be 0.02 nm.

3. Fabrication of the tunable fiber F-P filter and testing

The attenuation coefficient of the cobalt-doped optical fiber we used is 1 dB/cm from 1250 nm to 1620 nm. We did not choose cobalt-doped optical fibers with higher attenuation coefficient as low loss F–P cavity performs better. It is difficult to fabricate short FBG with high reflectivity in this cobalt doped fiber, more difficult than in ordinary single mode fiber. In order to enhance the photosensitivity, the cobalt doped fiber was hydrogen-loaded for one week (2–3 days is sufficient for ordinary SMF) at high temperature (about 100 °C) under 10 MPa pressure. The long time hydrogen loading leads to rich concentration of hydrogen in the fiber, even the micro-explosion could happen during fusion splicing process and makes the splicing failure. To overcome this problem we should first heat the fiber end to be spliced for several minutes and let the extra hydrogen go. The 2 mm long FBGs were fabricated by phase mask technology using a 193 nm ArF excimer laser, the

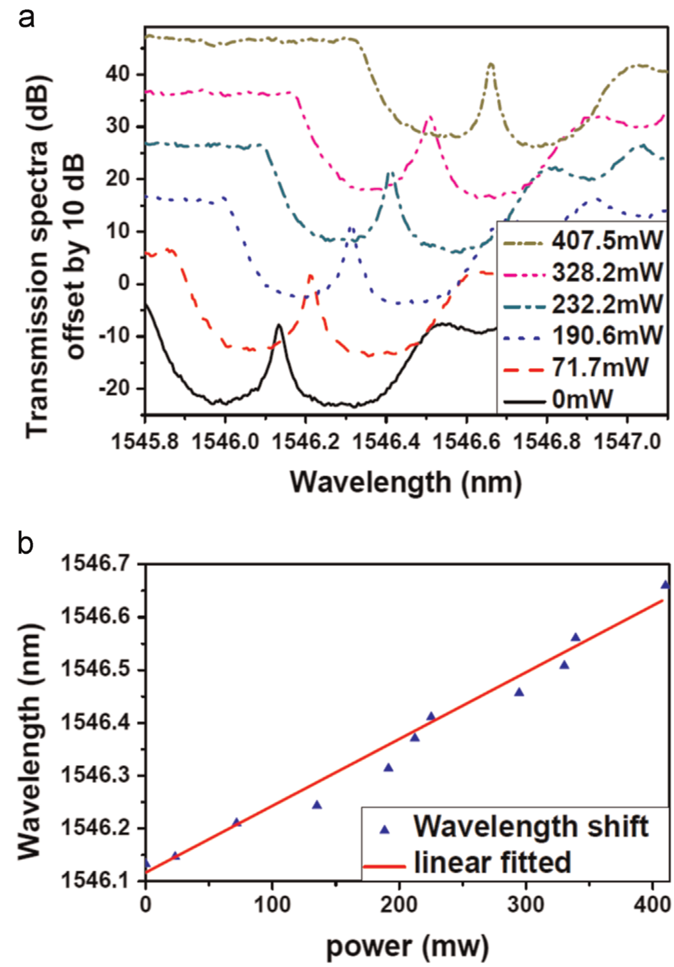

Fig. 4. Experiment results. (a) Transmission spectrum shifts with the increasing heating laser power. (b) The relationship of the transmission peak of the tunable fiber F–P filter and the heating power. The red curve is the linear fit. (For interpretation of the references to color in this figure legend, the reader is referred to the web version of this article.)

1 mm gap between the FBGP was controlled by a linear stage. The transmission spectrum was monitored in real time by OSA during fabrication. There is only one resonant peak in the range of the FBG bandwidth which indicates the single longitudinal mode operating property.

We tested the performance of the tunable fiber F–P filter using the setup shown in Fig. 1. The transmission peak exhibits a red shift as the heating laser power increases. Fig. 4a shows the shift of the tunable fiber F–P filter's transmission spectrum. The resonant peak shifts together with the envelope of the FBG's spectrum as they are in the same cobalt doped fiber. Fig. 4b shows the relationship between the shift of the resonant peak and the heating laser power. The peak shifts from 1546.133 nm to 1546.665 nm while the heating laser increased from 0 mW to 407.5 mW. The linear fit in Fig. 4b indicates the tuning coefficient is 1.27 pm/mW. The scan rate of our OSA is within 1 s, and the resonant peak stables within this time after changing the heating power. This is benefited from the small size of our F–P cavity as it is easy to achieve the thermal equilibrium. In this way, we successfully realized an all-optical fiber F–P filter, which is precisely tunable and has a narrow bandwidth about 0.02 nm.

The response time of the proposed filter is measured using the setup shown in the Fig. 5. The FBG interrogator (Micron Optics Inc., model: SM130) is for high speed spectrum analysis (250 Hz). The FBG interrogator is specially designed for measuring the reflection

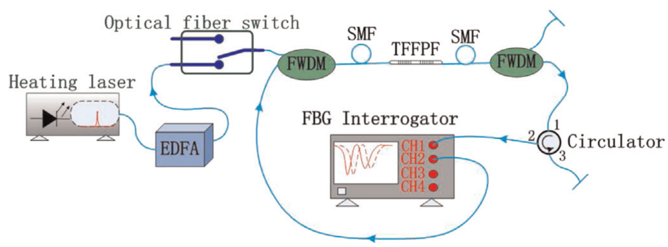

Fig. 5. Experiment setup for measuring the response time of the tunable F–P filter. The channel 2 of the FBG interrogator is used as light source and the channel 1 is for spectrum analysis. The sweep rate of the FBG Interrogator is 250 Hz and the modulation rate of the optical fiber switch is 0.05 Hz.

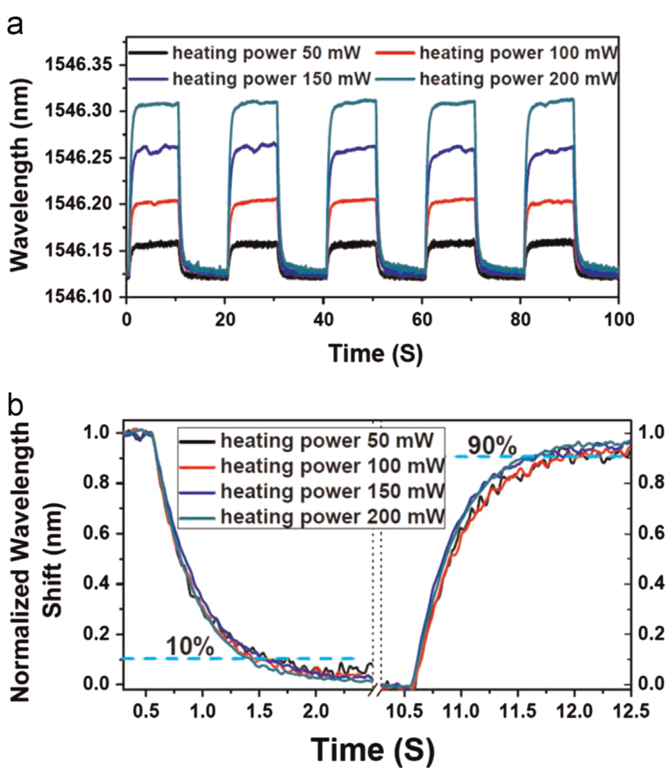

Fig. 6. The resonant wavelength shifts of the filter when the heating power is modulated at 0.05 Hz. (a) The wavelength shifts of the filter when the heating laser power is 50 mW, 100 mW, 150 mW and 200 mW, respectively. (b) The rise and fall time of the filter at different heating power when the wavelength shift is normalized.

spectrum of the FBGs. In order to measure the transmission spectrum of F–P filter, an optical fiber circulator is applied in this experiment, the channel 2 of the FBG interrogator is used as light source and the transmitted light is measured in channel 1. The heating laser is modulated by an optical fiber switch which is turned on and off every 10 s. The switching time is less than 8 ms which is fast enough for measuring the response time. The insertion loss of the switch is less than 0.5 dB. The wavelength shift of the resonant peak versus time is shown in Fig. 6. Fig. 6a shows the wavelength shifts at different heating power. In order to make these shifts comparable, the normalized wavelength shifts are shown in Fig. 6b. Although the wavelength shifts at different heating laser power are different, the normalized data show the rise and fall time are independent to the heating power. This result matches the thermal diffusion processes reported in the previous researches [20,21]. The rise and fall time is defined as the time the wavelength shift reaches 90% and 10% of the maximum value. They are estimated to be 1.25 s and 0.96 s in this experiment, which indicates the proposed tunable filter is practical in many slow variation systems.

4. Conclusion

In conclusion, we have made a tunable fiber F–P filter based on optically heated FBGs pair in cobalt fiber. We carefully designed the length of the FBGs and the cavity length to make sure the single longitudinal mode operation in the FBG's bandwidth. The 3 dB bandwidth of the filter is 0.02 nm. The resonant peak of the filter is controlled by the heating laser. Experimental results show the wavelength tuning coefficient is 1.27 pm/mW. This filter has an about 0.6 nm tuning range while the heating laser changes from 0 to 400 mw. The response time is measured using an FBG interrogator and an optical fiber switch. The rise and fall time of the filter is independent to the heating power and is estimated to be 1.25 s and 0.96 s. This high precision tunable narrow-band filter is a promising candidate in real applications such as optical fiber communication and optical fiber sensing systems.

Acknowledgments

This work was supported by the National Natural Science Foundation of China (No. 61307053) and China Postdoctoral Science Foundation (No. 2013M531866).

References

[1] K. Zhou, X. Chen, L. Zhang, I. Bennion, High-sensitivity optical chemsensor based on etched D-fibre Bragg gratings, Electron. Lett. 40 (2004) 232.
[2] D. Chen, W. Liu, M. Jiang, S. He, High-resolution strain/temperature sensing system based on a high-finesse fiber cavity and time domain wavelength demodulation, J. Lightwave Technol. 27 (2009) 2477–2481.
[3] Wei Liang, Yanyi Huang, Yong Xu, Reginald K. Lee, Amnon Yariv, Highly sensitive fiber Bragg grating refractive index sensors, Appl. Phys. Lett. 86 (2005) 151122.
[4] X.P. Cheng, P. Shum, C.H. Tse, J.L. Zhou, M. Tang, W.C. Tan, R.F. Wu, J. Zhang, Single-longitudinal-mode erbium-doped fiber ring laser based on high finesse fiber Bragg grating Fabry–Perot etalon,, IEEE Photon. Technol. Lett. 20 (12) (2008) 976–978.
[5] D. Chen, H. Fu, W. Liu, Y. Wei, S. He, Dual-wavelength single longitudinal-mode erbium-doped fiber laser based on a fiber Bragg grating pair and its application in microwave signal generation,, Electron. Lett. 44 (7) (2008) 459–461.
[6] F.T.S. Yu, S. Yin, Fiber Optic Sensors, Dekker, New York (2002) 124 (Chaps. 2 and 4).
[7] Y.J. Rao, Recent progress in applications of in-fibre Bragg grating sensors, Opt. Lasers Eng. 31 (1999) 297–324.
[8] A. Wada, S. TanakaN. Takahashi, High-sensitivity vibration sensing using in-fiber Fabry–Perot interferometer with fiber-Bragg grating reflectors, Tech. Digest OFS 20 (2009) 75033L-1-75033L-4.
[9] T.T.-Y. Lam, J.H. Chow, D.A. Shaddock, I.C.M. Littler, G. Gagliardi, M.B. Gray, D. E. McClelland, High-resolution absolute frequency referenced fiber optic sensor for quasi-static strain sensing, Appl. Opt. 49 (2010) 4029–4033.
[10] Y.N. Ning, A. Medrum, W.J. Shi, B.T. Meggitt, A.W. Palmer, K.T.V. Grattan, L. Li, Bragg grating sensing instrument using a tunable Fabry–Pérot filter to detect wavelength variations, Meas. Sci. Technol. 9 (1998) 599–606.
[11] K. Liu, W.C. Jing, G.D. Peng, J.Z. Zhang, D.G. Jia, H.X. Zhang, Y.M. Zhang, Investigation of PZT driven tunable optical filter nonlinearity using FBG optical fiber sensing system, Opt. Commun. 281 (2008) 3286–3290.
[12] Ping Ge, Musa Jouaneh, Modeling hysteresis in piezoceramic actuators, Precis. Eng. 17 (1995) 211–221.
[13] Markus Schmidt, Bernd Werther, Norbert Fürstenau, Fiber-optic extrinsic Fabry–Perot interferometer strain sensor with < 50 pm displacement resolution using three-wavelength digital phase demodulation, Opt. Express 8 (8) (2001) 475–4480.
[14] Monica K. Davis, Michel J.F. Digonnet, Measurements of thermal effects in fibers doped with cobalt and vanadium, J. Lightwave Technol. 18 (2) (2000) 161–165.
[15] John A. Rogers, Benjamin J. Eggleton, Rebecca J. Jackman, Glen R. Kowach, Thomas A. Strasser, Dual on-fiber thin-film heaters for fiber gratings with independently adjustable chirp and wavelength, Opt. Lett. 24 (19) (1999) 1328–1330.
[16] A.K. Ahuja, P.E. Steinvurzel, B.J. Eggleton, J.A. Rogers, Tunable single phase-shifted and superstructure gratings using microfabricated on-fiber thin film

heaters, Opt. Commun. 184 (2000) 119–125.
[17] Z. Zhao, Y. Yu, S. Zhang, Z. Zhuo, J. Zhang, W. Zheng, Y. Zhang, Adjustment of the central wavelength and the chirp of fiber Bragg grating separately with external heaters, Opt. Commun. 242 (1) (2004) 135–139.
[18] Yang Zhang, Bai-Ou Guan, Hwa-Yaw Tam, Ultra-short distributed Bragg reflector fiber laser for sensing applications, Opt. Express 17 (12) (2009) 10050–10055.
[19] Y.O. Barmenkov, D. Zalvidea, S.T. Peiro, J.L. Cruz, M.V. Andres, Effective length of short Fabry–Perot cavity formed by uniform fiber Bragg gratings, Opt. Express 14 (14) (2006) 6394–6399.
[20] H.H. Bruun, Hot-Wire Anemometry: Principles and Signal Analysis, Oxford University Press Inc., New York, 1995.
[21] Zhengyong Liu, Ming-Leung Vincent Tse, A. Ping Zhang, Hwa-Yaw Tam, Integrated microfluidic flowmeter based on a micro-FBG inscribed in Co^{2+}-doped optical fiber, Opt. Lett. 20 (2014) 5877–5880.